Rev. Adv. Mater. Sci. 31 (2012) 116-122

EFFECT OF HIGH STRAIN RATE PROCESSING ON STRENGTH AND DUCTILITY OF ULTRAFINE-GRAINED Cu PROCESSED BY EQUAL CHANNEL ANGULAR PRESSING

Y.C. Dong[1,3], Y. Zhang[2], I.V. Alexandrov[1] and J.T. Wang[3]

[1]The Department of Physics, Ufa State Aviation Technical University, 12, K. Marx, Ufa 45000, Russia
[2]Key Laboratory for Materials Modification by Laser, Ion and Electron Beam (Ministry of Education), Dalian University of Technology, Dalian, 116024, PR China
[3]School of Materials Science and Engineering, Nanjing University of Science and Technology, Nanjing, Jiangsu 210094, PR China

Received: April 20, 2012

Abstract. Bimodal microstructure consisting of ultrafine-grained (UFG) matrix with the embedded micro-size recrystallized grains has been developed in Cu due to equal channel angular pressing (ECAP) and subsequent high strain rate deformation (HSRD). Both high strength and high ductility are characteristic for this microstructure. High strength is achieved by grain refining with high density of high-angle grain boundaries, developed during the ECAP. High ductility is the result of the appearance of dynamically recrystallized grains generated during the HSRD.

1. INTRODUCTION

The methods of severe plastic deformation (SPD) have widely been developed during the last few years. This fact has allowed to attain a high deformation strain e >10 in metallic materials and leads to significant high strength, simultaneously preserving the size of the deformed billets unchanged [1, 2]. Special plastic deformation schemes have been designed to provide shear stress under high hydrostatic pressure, which have provided a possibility to refine the microstructure of metals down to the level of ultrafine-grained (UFG) (100-1000 nm) size or a nanostructured (NS) (below 100 nm) size with high angle grain boundaries (GBs). High pressure torsion (HPT) and equal channel angular pressing (ECAP) are the most effective SPD methods.

In comparison with the coarse grained materials, the UFG/NS billets usually possess high strength but low ductility. Thereby, the urgent subject of the research is improving the ductility of the UFG/NS materials currently. There are several approaches based on microstructure control aiming at solving this problem. They include the development of the bimodal microstructure [3], the formation of high density of non-equilibrium high angle grain boundaries [4], the generation of ultrahigh density of nano-scaled twins [5] and the introduction of a gradient grain-sized distribution in microstructure [6]. On the other hand, the optimized mechanical properties have been achieved by various technical methods, for instance, the dynamic equal channel angular pressing (DECAP) [7,8], the dynamic plastic deformation (DPD) [9] and the composite processing methods (ECAP + cryodrawing + cryorolling) [10]. However, low reproducibility, high complexity of the processing technology and limited size of a billet are the shortcomings of these methods.

The dynamic behavior of UFG Cu processed by the ECAP has been investigated in our primary re-

Corresponding author: I.V. Alexandrov, e-mail: iva@mail.rb.ru

search [11]. Dynamically recrystallized grains had been observed in the microstructures of the samples after large number of the ECAP passes. Resting upon the absence of adiabatic shear bands and cracks, one can suggest that effective bimodal microstructure consisting of UFG/NS matrix with the embedded dynamically recrystallized micron-sized grains is resulted from the ECAP and subsequent HSRD procedures. Considering that the UFG/NS matrix would be responsible for high strength and dynamically recrystallized micron-sized grains would be responsible for the ductility, the aim of the present investigation is to study the effect of a high strain rate processing on strength and ductility of ultrafine-grained Cu processed by the ECAP.

2. EXPERIMENTAL

The investigated material was bulk OFHC Cu (99.98%). Before ECAP the ingots were annealed at 873K for 1 h under vacuum atmosphere in order to remove the internal residual strain. After annealing the obtained coarse-grained (CG) microstructure had the grain size equal to 90 μm. 1, 4, and 8 ECAP passes by route B_C were carried out at room temperature [12]. The ECAP die was designed with an internal channel angle equal to 90° and an external arc angle equal to 20°. The dimension of the ECAP ingots was 12 mm × 12 mm × 100 mm.

Cylindrical specimens with dimension ∅ 10×10 mm were cut out along the ECAP direction and subjected to high strain rate deformation (HSRD). The HSRD was performed using Split Hopkinson Pressure Bar setup at room temperature with high strain rate approximately equal to 1500 s^{-1}. The tensile tests of the ECAP (Cu_{ECAP}) and the ECAP + HSRD ($Cu_{ECAP+HSRD}$) samples were carried out on a tensile testing machine with a quasi-static strain rate of 2×10^{-3} s^{-1} at room temperature. The samples had a 1 mm × 0.5 mm cross-section and a 4 mm gauge length.

Microstructural characterization of Cu samples before the tensile tests was performed by the method of optical microscopy (OM). Before carrying out the OM investigation, the samples were mechanically polished by the abrasive paper and diamond polishing paste, then etched in a solution of 70% nitric acid and 30% ethanol. TEM analysis was carried out on a JEOL JEM-2100, which was operating at an acceleration voltage of 200 kV. The specimens with diameter of 3 mm for the TEM examination were obtained from the same longitudinal section. After polishing the disks, thin foils were prepared for the TEM examination using a twin-jet Tenupol-3 polisher with an electro-polishing solution composed of volume 1:2 nitric acid and methanol at room temperature. After the tensile test the microstructural characterization of Cu samples was performed on a JSM-6390 scanning electron microscope (SEM). Fracture morphology was analyzed on the corresponding vertical and horizontal surfaces.

3. RESULTS AND DISCUSSION

The tensile engineering quasi-static deformation curves for the CG, CG_{HSRD}, and $UFG_{ECAP+HSRD}$ Cu

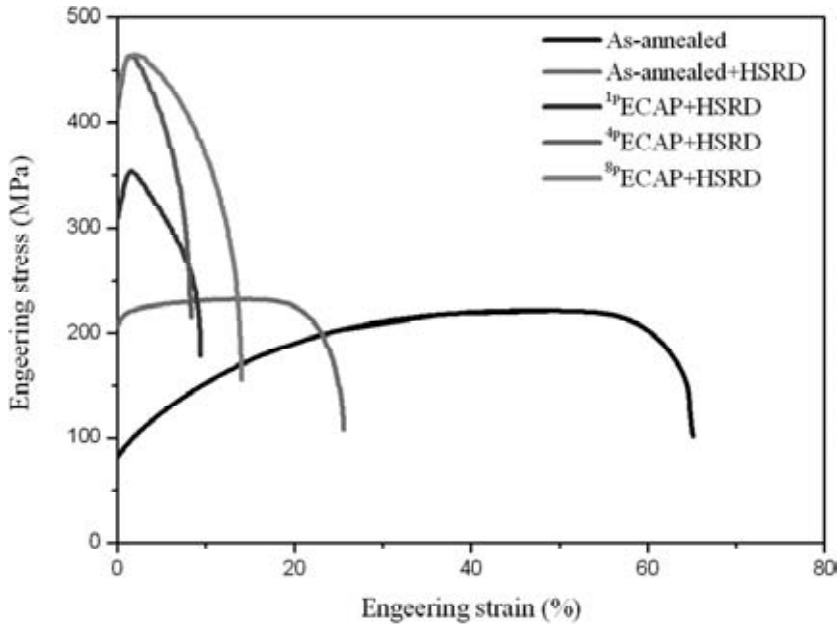

Fig. 1. Engineering stress-strain curves for as-annealed, as-annealed and ECAP Cu after HSRD.

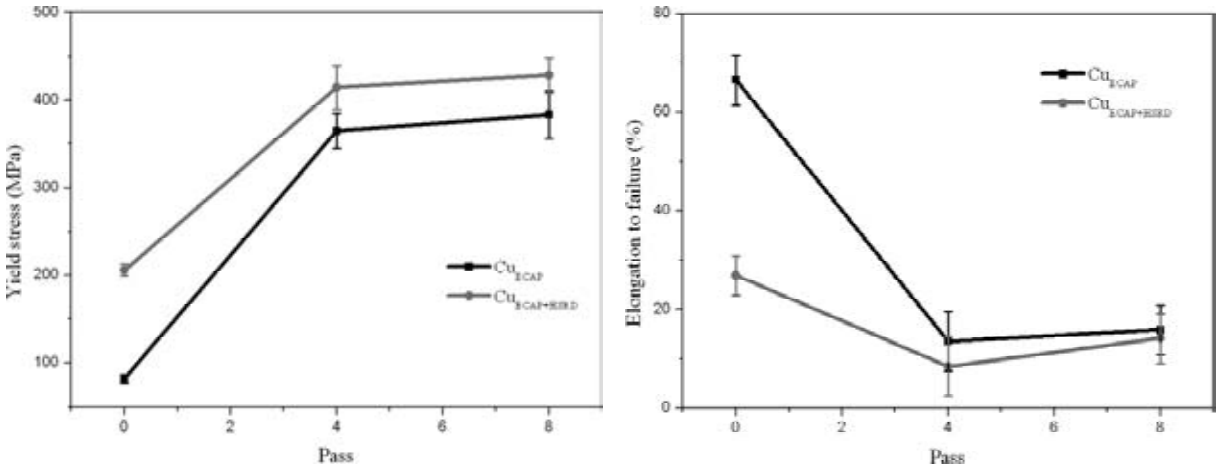

Fig. 2. The mechanical behaviors of Cu_{ECAP} and $Cu_{ECAP+HSRD}$ samples vs. different number ECAP passes. (a) yield stress, (b) elongation to failure.

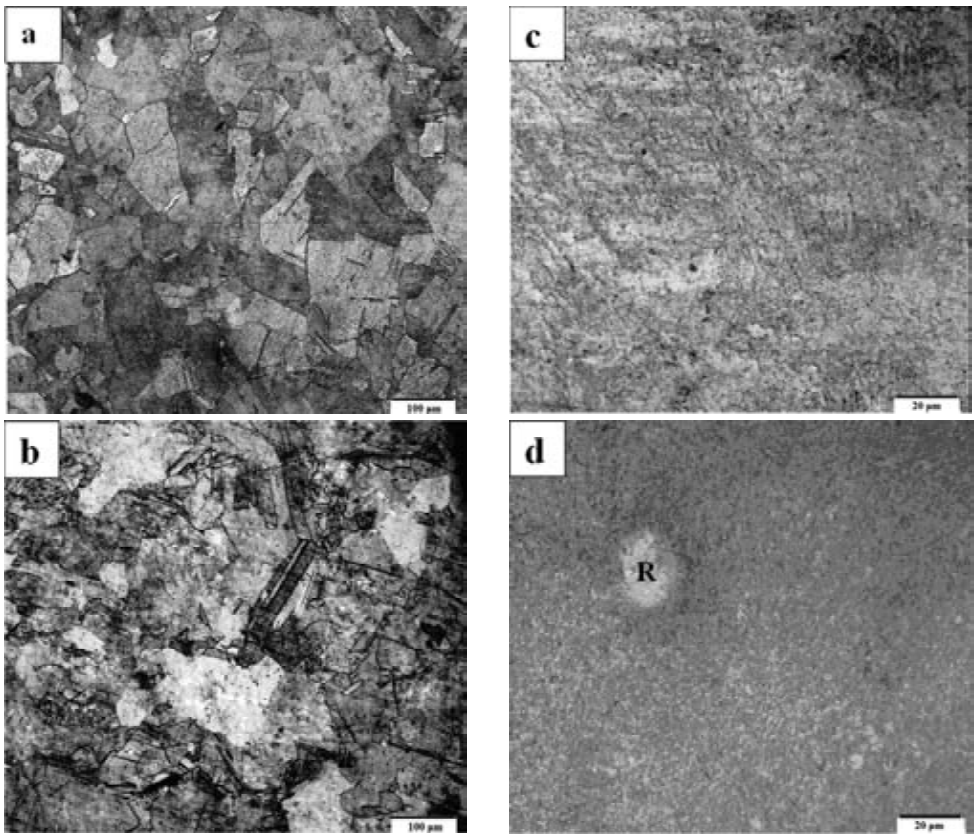

Fig. 3. Optical microscopy images: (a) CG Cu, (b) CG_{HSRD} Cu, (c) $Cu_{4pECAP+HSRD}$, (d) $Cu_{8pECAP+HSRD}$.

samples are shown in Fig. 1. For the CG_{HSRD} Cu the flow stress reaches 206 MPa, which is more than twice higher than that of the CG Cu. On the other hand, the ductility decreases dramatically with the reduction of strain hardening. For the $UFG_{1pECAP+HSRD}$ Cu the yield strength increases up to 309 MPa and the value reaches 414 MPa for the $UFG_{4pECAP+HSRD}$ Cu with the continuous loss of ductility. This tendency reverses for the $UFG_{8pECAP+HSRD}$ Cu, which has a yield strength reinforcing to 428 MPa and ductility recovering to ~15%. In comparison with the results of $Cu_{ECAP+HSRD}$ and Cu_{ECAP} we can clearly notice that the HSRD method enables to strengthen the UFG_{ECAP} Cu and to keep the ductility (Fig. 2).

Strength and ductility are often regarded as mutually exclusive parameters, which means, if one of them increases, the other one decreases simultaneously. The earlier investigations of the bimodal distribution microstructure [3,9] have shown that the

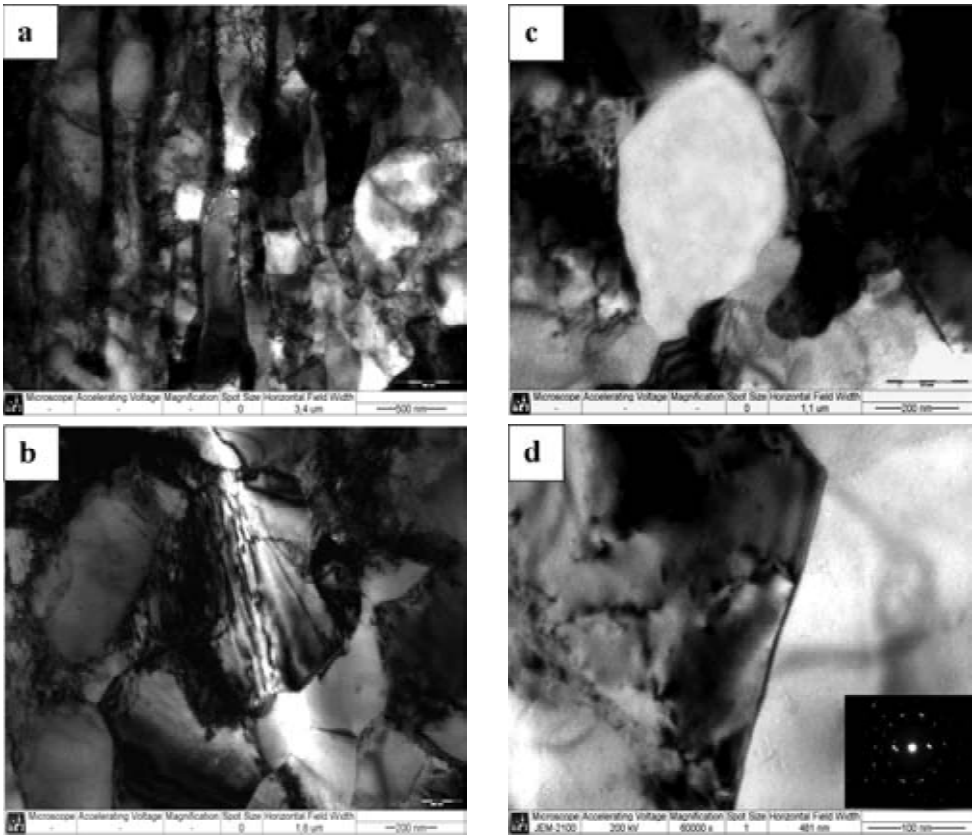

Fig. 4. TEM microstructures for $Cu_{4ECAP+HSRD}$: (a) lamellar dislocation bands (LBs), (b) dislocations in grains and boundaries, (c) recrystallized grain, (d) a boundary of recrystallized grain and the selected area diffraction pattern.

ductility can be improved by static annealing, but such an increase inevitably results in the loss of strength. Our research revealed that both the optimized strength and ductility could be achieved in the result of the temperature rise during the high strain rate deformation.

Mechanical properties of materials are determined by their microstructures. Fig. 3 indicates the optical microstructures of CG, CG_{HSRD}, $UFG_{4ECAP+HSRD}$, and $UFG_{8ECAP+HSRD}$ samples. The as-annealed sample displays a structure with clear and straight grain boundaries as well as several annealing twins (Fig. 3a). The average grain size is about 90 μm. After the HSRD pressing the initial grains of CG microstructure were broken into pieces and messed up. The image reflects a diffusive microstructure with the corrugated grain boundaries and plenty of deformation twins (Fig. 3b), which are conventionally generated in Cu at high strain rates or low temperatures. The deformation twins hinder the slip of dislocations, this fact can increase the strength. For the $UFG_{4pECAP+HSRD}$ sample the grains are too small to recognize, but it also displays an inhomogeneous microstructure (Fig. 3c). The recrystallized grains which are embedded into the UFG matrix are obviously observed in the microstructure of $UFG_{8pECAP+HSRD}$ sample. Some of these grains even approach to ~10 μm as the result of the secondary recrystallization (Fig. 3d, marked as R).

The TEM investigations of the $UFG_{4pECAP+HSRD}$ sample (Fig. 4) have indicated a microstructure with lamellar dislocation bands (LBs) (Fig. 4a). The dislocations in grain interiors, grain boundaries and sub-boundaries (Fig. 4b) contribute to the high strength (up to ~465 MPa) of the samples, which is much higher than that of the UFG_{4pECAP} sample (~ 420 MPa). One recrystallized grain with a size of ~500 nm, which has dislocation-free interior and well-defined boundaries, is obviously observed in the $UFG_{4pECAP+HSRD}$ Cu (Fig. 4c). Fig. 4d clearly displays the movement of dislocations towards the grain boundary and the dislocation absorption by it. The sharp and clear grain boundary image indicates the occurrence of the dynamic recrystallization in the microstructure, where the dislocation tangles are disappearing and grain boundaries with high misorientation angles are being formed. The diffraction spots of SAD pattern indicate a high angle

misorientation of ~ 15° between left and right grains (Fig. 4d).

For metals the high strain rate deformation is the adiabatic process, which is always accompanied with heat generation, transformed from 90% of the deformation work. The remained 10% are stored in defects of the deformed materials [13]. The elevated temperature (ΔT_d) in the split Hopkinson bar test corresponding to this heat generation can be expressed as a function of stress and strain [14]:

$$\Delta T_d = \frac{\beta}{\rho C_p}\int_{\varepsilon_0}^{\varepsilon_1} \sigma \cdot d_\varepsilon, \quad (1)$$

where ρ is the density of material, C_p is the heat capacity, and β is the Taylor factor, i.e. the fraction of the energy obtained from the deformation work. Using Johnson-Cook equation [15] as the constitutive equation for the response, the temperature increase due to high strain rate deformation can be expressed as the equation [16]:

$$\Delta T_d = 1 - \left[\frac{-0.9\left[1 + C\log\frac{\dot{\varepsilon}}{\dot{\varepsilon}_0}\right]}{\rho C_p\left(T_m - T_r\right)} \times \left[\sigma_0\varepsilon + \frac{B\varepsilon^{n+1}}{n+1}\right]\right], \quad (2)$$

where T_r is the room temperature, T_m is the melting temperature, B, C are the constants of hardening and strain rate, n is the hardening exponent. For the cylindrical samples for compression, the temperature of the sample is directly proportional to $\dot{\varepsilon}$ and ε.

According to the calculations of Mishra *et al*. [17], a dynamic recrystallization takes place at the calculated temperature 360K in the UFG Cu during the impact. This temperature is much lower than the one, related to the static recrystallization of Cu (476K for the 99.98% Cu after 8 passes ECAP deformation [18]). It needs to be noticed that recrystallization temperature decreases with the increasing purity of Cu [19]. Murr *et al*. [20-23] have carried out extensive experiments on dynamic recrystallization induced by high strain rate plastic deformation in both ballistic impact and friction stir-welding. The associate link of the recrystallization with the dynamic deformation process is undeniable in the process of SPD. The strain of $UFG_{4pECAP+HSRD}$ and $UFG_{8pECAP+HSRD}$ samples is almost the same value of 0.2~0.3 [11]. Hereby, the generation of heat is supposed to be the same at fixed strain rate for these two samples. So, the reason which has led to the revealed differences in the microstructure of these two samples came from the ECAP process.

The SPD samples always undergo a significant shear strain during their fabrication. For the ECAP process, the strain can be defined by the equation [24]:

$$\varepsilon_N = N\left[\frac{2\cot\left(\varphi/2 + \psi/2\right)}{\sqrt{3}} + \frac{\psi\csc\left(\varphi/2 + \psi/2\right)}{\sqrt{3}}\right], \quad (3)$$

where N is the number of ECAP passes, φ and ψ represent internal and external angles of the ECAP die respectively. In our research each additional pass adds the strain ~1 to the cumulative strain. The dislocation generation and additional grain refinement takes place here. Many investigators [4,10] have reported the observations of a high density of high angle grain boundaries generated after a large number of the ECAP passes. The activation energy of recrystallization is low in severely deformed samples, which makes the recrystallization easier in the UFG_{4pECAP} sample and accelerates it in the UFG_{8pECAP} Cu. Thereby, in the present research the high density of high-angle boundaries processed by the ECAP deformation and recrystallized grains formed during the HSRD can improve the ductility of the UFG Cu.

Fig. 5 shows the appearance of fracture morphologies for the $UFG_{ECAP+HSRD}$ samples. The $UFG_{8pECAP+HSRD}$ sample obviously shows a narrow neck plane before fracture, which proves a better ductility (Fig. 5d). In the $UFG_{1pECAP+HSRD}$ (Fig. 5a) and the $UFG_{4pECAP+HSRD}$ (Fig. 5b) samples the fracture surfaces display the same morphology. However, in the second case a cleavage fracture area can be observed in the microstructure. This results in the lowest ductility of the $UFG_{4pECAP+HSRD}$ Cu sample (Fig. 5c) among all the others.

Wang *et al.* [3] has used cold rolling to produce UFG/NS samples, which exhibit the same mechanical properties as the samples in the present research, then quasi-static annealing was conducted to produce recrystallized grains and to improve ductility. Valiev *et al.* [4] have also done an incredible work to optimize the mechanical properties by generation of high density of high-angle grain boundaries. In our investigation we have successfully developed a feasible way to enhance the strength of UFG/NS Cu with improved ductility. This follows from the application of the HSRD method which forms the recrystallized grains in the UFG/NS matrix due

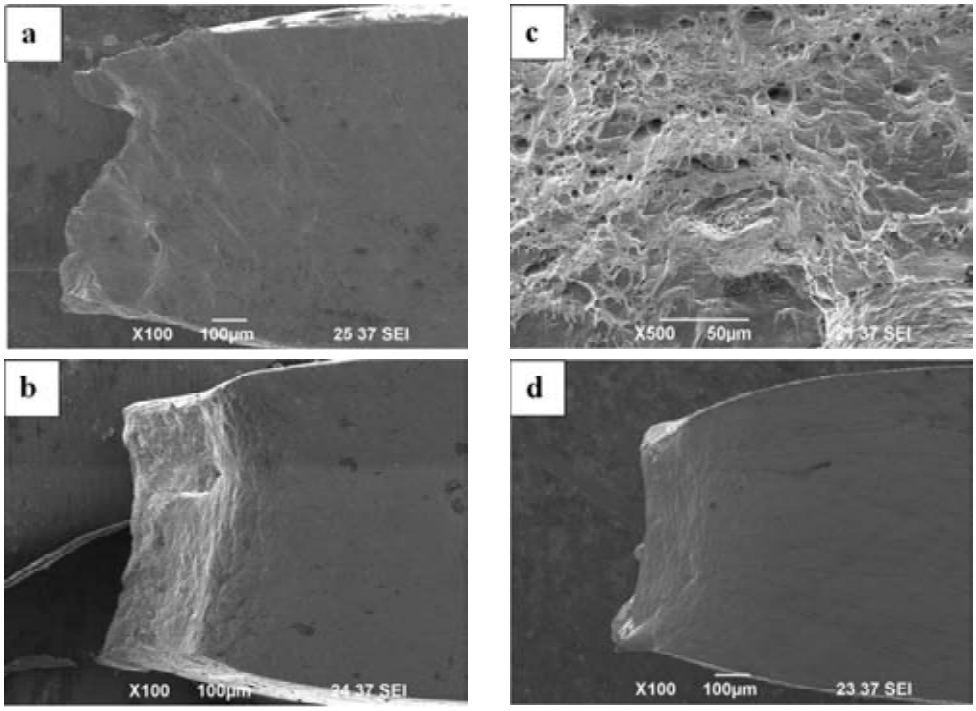

Fig. 5. Fracture morphology after tensile tests of (a) $UFG_{1pECAP+HSRD}$ Cu, (b) $UFG_{4pECAP+HSRD}$ Cu, (c) high magnification of $UFG_{4pECAP+HSRD}$ Cu, (d) $UFG_{8pECAP+HSRD}$ Cu.

to some elevation of temperature during the deformation. As a result, the strength and ductility increase simultaneously.

ACKNOWLEDGEMENT

This work was supported by the Key scientific research Project of the Ministry of Education of China under grant no. 311035.

REFERENCES

[1] R.Z. Valiev, R.K. Islamgaliev and I.V. Alexandrov // *Prog. Mater. Sci.* **45** (2000) 103.
[2] R.Z. Valiev and T.G. Langdon // *Prog. Mater. Sci.* **51** (2006) 881.
[3] Y.M. Wang, M.W. Chen, F.H. Zhu and E. Ma // *Nature* **419** (2002) 912.
[4] R.Z. Valiev, I.V. Alexandrov, Y.T. Zhu and T.C. Lowe // *J. Mater. Res.* **17** (2002) 5.
[5] L. Lu, Y. F. Shen, X.H. Chen, L.H. Qian and K. Lu // *Science* **304** (2004) 422.
[6] T.H. Fang, W.L. Li, N.R. Tao and K. Lu // *Science* **331** (2011) 1587.
[7] S. Shekhar, J. Cai, J. Wang and M.R. Shankar // *Mater. Sci. and Eng. A*. **527** (2009) 187.
[8] I.V. Khomshaya, E.V. Shorokhov, V.I. Zel'dovich, A.E. Kheifets, N.Yu. Frolova, P.A. Nasonov, A.A. Ushakov and I.N. Zhgilev // *The Physics of Met. and Metall*. **111** (2011) 612.
[9] W.S. Zhao, N.R. Tao, J.Y. Guo, Q.H. Lu and K. Lu // *Scripta Mater*. **53** (2005) 745.
[10] Y.H. Zhao, J.F. Bingert, X.Z. Liao, B.Z. Cui, K. Han, A.V. Sergueeva, A.K. Mukherjee, R.Z. Valiev, T.G. Langdon and Y.T. Zhu // *Adv. Mater*. **18** (2006) 2949.
[11] Y.C. Dong, I.V. Alexandrov and J.T. Wang // *Mater Science Forum* **667** (2011) 891.
[12] M. Furukawa, Y. Iwahashi, Z. Horita, M. Nemoto and T.G. Langdon // *Mater. Sci. and Eng. A.* **257** (1998) 328.
[13] M.A. Meyers, *Dynamic Behaviour of Materials* (National Defence Industry Press, New York, (1994), p. 260.
[14] M.A. Meyers, J.C. LaSalvia, V.F. Nesterenko, Y.J. Chen and B.K. Kad In: *McNelley TR*, ed. by Rex '96 (Monterey 1997), p. 27.
[15] G.R. Johnson and W.H. Cook In: *Proceedings of the 7th international symposium on ballistics* (The Netherlands 1983).
[16] D.H. Lassila, T. Shen, B.Y. Cao and M.A. Meyers // *Metal Mater. Trans*. **35A** (2004) 2729.
[17] A. Mishra, M. Martin, N.N. Thadhani, B.K. Kad, E.A. Kenik and M.A. Meyers // *Acta Mater* **56** (2008) 2770.
[18] Y. Zhang, J.T. Wang, C. Cheng and J.Q. Liu // *J. Mater. Sci.* **43** (2008) 7326.

[19] W. Gao, A. Belyakov, H. Miura and T. Sakai // *Mater. Sci. and Eng. A.* **265** (1999) 233.
[20] L.E. Murr, A. Trillo, S. Pappu and C. Kennnedy // *J. Mater. Sci.* **37** (2002)3337.
[21] L.E. Murr and E.V. Esquivel // *J. Mater. Sci.* **39** (2004)1153.
[22] E.V. Esquivel and L. E. Murr // *Mater. Sci. Tech*. **22** (2006) 438.
[23] L.E. Murr and C. Pizana // *Met. Mater. Trans*. **38A** (2007) 2611.
[24] Y. Iwahashi, J.T. Wang, Z. Horita, M. Nemoto and T.G. Langdon // *Scripta Mater*. **35** (1996) 143.